New AOTF-based instrumental concepts for atmospheric science

Emmanuel Dekemper[*a], Jurgen Vanhamel[a], Jean-Claude Kastelik[b], Nuno Pereira[a], David Bolsée[a], Gael Cessateur[a], Hervé Lamy[a], Didier Fussen[a]
[a]Royal Belgian Institute for Space Aeronomy (BIRA-IASB), 3 avenue Circulaire, Belgium;
[b]Université Polytechnique des Hauts-de-France, CNRS, Univ. Lille, YNCREA, Centrale Lille, UMR 8520 IEMN, DOAE, 59313 Valenciennes, France

ABSTRACT

Acousto-optical tunable filters (AOTFs) are still little known to the Earth atmosphere remote sensing community. The bulk of passive atmospheric remote sensing instruments remains divided into two families: those relying on interferometric techniques (mostly for the long-wave absorbing species), and those based on diffraction gratings (better suited for UV-VIS absorbing species).

Still, AOTFs have some unique features which should deserve more attention, in particular their angular acceptance, and their polarization sensitivity. The first one because it allows to work in an imaging setup, the second because many atmospheric processes have a polarizing effect.

In this paper, we will present different AOTF-based instrument concepts (or even prototypes) which take advantage of these features in order to improve the sate-of-the-art of measurement techniques in several fields of atmospheric science. We will first present the improved NO_2 camera: its new capabilites, the subsystems which have been changed, and some preliminary results. Then, we will discuss two other potential applications: the study of the solar spectral irradiance variability in the UV, and the detection of auroral polarized emissions.

For each concept, we will discuss the current challenges faced by the existing instruments, and analyze how the use of AOTFs could overcome them. A suggestion for the AOTF selection will be made, and the expected instrument performance will be estimated.

Keywords: AOTF, acousto-optic, atmosphere, remote sensing, aurora, solar spectral irradiance, nitrogen dioxide, NO2

1. INTRODUCTION

According to our knowledge, only three AOTF-based instruments aiming at the measurement of atmospheric parameters are being developed: ALTIUS[1], a satellite-borne hyperspectral imager for the monitoring of the ozone layer, the NO_2 camera[2], an offspring of ALTIUS optimized for the measurement of industrial NO_2 emissions, and ALI[3], also inspired by ALTIUS, flown on stratospheric balloons to measure aerosol extinction profiles.

Despite this small number of applications, AOTFs have a number of advantages which can make them an attractive option for instruments seeking a fast and robust tunable filter capable of processing bidimensional light fields with a high sensitivity to the polarization.

In this paper, we will first focus on the NO_2 camera, as it will be the baseline for the two other instrumental concepts that we would like to introduce. We will recall the original concept, and present how it has been improved to get closer from an operational air pollution monitoring instrument.

Not yet prototyped, but nonetheless promising are the two other instrumental concepts: one for the measurement of the solar spectral irradiance variability in the UV, the other for the quantification of the degree of linear polarization of some auroral emission lines in the visible domain. For these two, we will summarize the current difficulties faced by past and existing instruments, then propose an AOTF-based solution potentially overcoming these issues.

[*] Corresponding author: emmanuel.dekemper@aeronomie.be.

Fourteenth School on Acousto-Optics and Applications, edited by Ireneusz Grulkowski, Bogumił B. J. Linde, Martí Duocastella, Proc. of SPIE Vol. 11210, 112100S
 · doi: 10.1117/12.2540981

2. THE IMPROVED NO_2 CAMERA FOR THE MONITORING OF URBAN AIR POLLUTION

Fossil fuel combustion (heating, transport) is the main source of NO_x ($NO+NO_2$) in the boundary layer of the atmosphere. NO_2, in particular, is harmful for lung and causes a series of health problems. A number of policies aiming at reducing exposure to NO_x have been (are being) put in place at various levels, but the urban scale is probably the most meaningful.

The monitoring of the concentration of NO_x is classically performed by a limited number of in situ air samplers which can be very accurate for the neighboring air parcel but which do not constitute a sufficiently dense network to allow forecasting the concentration of NO_x at street level across the city. What is missing, is a network of instruments overseeing the city from a small number of locations in order to 3-D sample the NO_x field with a temporal resolution of an hour, and a street level spatial resolution.

Some of the authors of this work have demonstrated an instrumental concept[2], based on AOTFs, which is capable of monitoring the NO_2 emissions of point sources like coal-firing power plants. Since then, the prototype has been improved in almost every aspects. Table **1** lists the main improvements. Figure **1** shows the current instrument in the laboratory.

Table 1: Comparison of key parameters between the original NO_2 camera, and the improved one.

	Parameters of the initial NO_2 camera	**Parameters of the improved NO_2 camera**
AOTF type	TeO_2, noncollinear, cut angle: 7.6°, linear aperture: 10x10mm², Δλ=0.7nm (at 450nm)	same
Sensor	Princeton instrument Pixis 512B CCD, 512x512 pixels	Hamamatsu CMOS, 2048x2048 (binned 4X4 to yield a 512x512 image)
RF generation	lab equipment: R&S Signal Generator SMT-02 and AR Amplifier	In-house designed redundant RF generators based on the AD9910 DDS of Analog Devices and the ADF4108 PLL of Analog Devices, both connected to the ZHL-2-8-S+ RF amplifier of MiniCircuits
Bandpass filter	none	425-475 nm
Field of view	6°x6°	20°x20°
Energy source	220V, 100 W	24V, 20 W
Control software	labview	python code

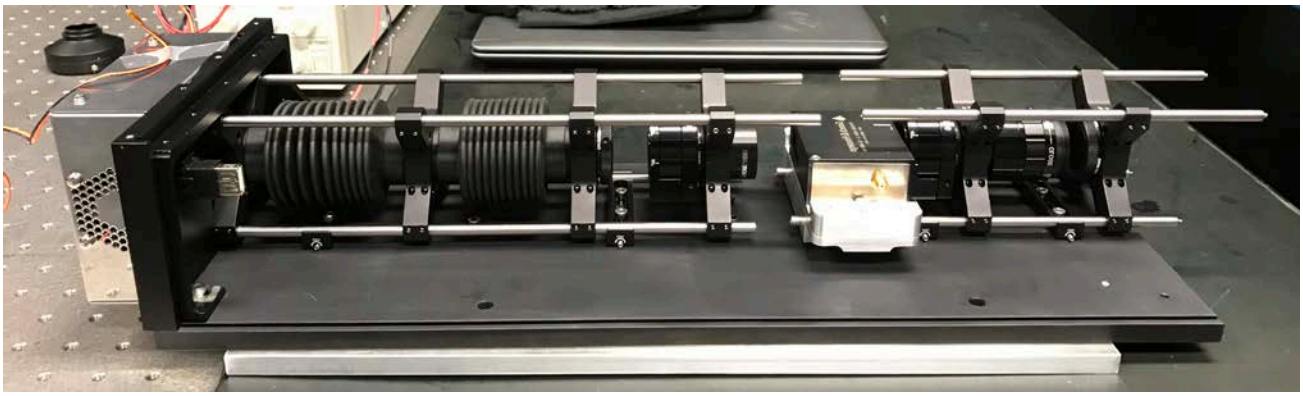

Figure 1: The improved NO_2 camera: on the left, the CMOS sensor housing, close to the middle, the AOTF surrounded by two cross-oriented polarizers.

The optical layout is also similar: a telecentric front-end optical (FEO) system ensures a high spectral purity of the image by preserving the light incidence angle across the AOTF aperture[4], while the back-end optics (BEO) is responsible for

imaging the diffracted order of the AOTF onto the detector. Optical and opto-mechanical parts are off the shelf but have all been changed, primarily to increase the field of view (FOV) from 6°x6° to 20°x20°, and also to match the new sensor size. A bandpass filter has been inserted in order to keep the part of the natural light spectrum which provides the largest sensitivity to NO_2: the region around 450 nm. Only the TeO_2 AOTF has been re-used. See reference [2] for a description.

In the first designed breadboard, the generation of the RF signal to drive the AOTF was done using bulky lab equipment. A trade-off analysis for a printed circuit board solution led to the selection of two RF chains: one based on Phase Locked Loop (PLL) approach, and another one on Direct Digital Synthesis (DDS). In addition, a market study was carried out for the RF amplifier in order to select the most appropriate device. The amplifier capable of delivering the requested output power was found off the shelf at MiniCircuits. More details on the optimization process can be found in reference [5].

A limitation of the previous concept was the low frame rate. Indeed, observing moving targets such as smokestack plumes requires a speed of acquisition consistent with the dynamics of the target (puffs, changing wind, etc). Achieving this imposed a number of improvements:

1. The CCD was replaced by a CMOS (Hamamatsu C11440-52U) which, in addition to offering at least a 30Hz frame rate at full spatial resolution, also comes with a number of other benefits: a much lower power consumption (no cooling), a small volume, low noise, and USB 3.0 interface among others.
2. The control software was re-developed in Python and is capable of steering the RF generation, triggering image acquisition, and reading out the data with as less dead time as possible.
3. The spectral image acquisition scenario was revised to allow for looping through the desired wavelengths with a short exposure time (typically 100 ms). After a while, images are sorted per wavelength and co-added in order to increase the signal-to-noise ratio of the monochromatic images. This avoids to have inconsistencies among the different wavelengths caused by a potential change of the scene between two spectral images.

Another essential improvement is the use of temperature-dependent elastic coefficients[6] and refractive indices[7] for TeO_2. Based on these values, the theoretical tuning curve of the AOTF reveals that a change of 1K yields a shift of 0.1 nm in the filtered wavelength (at constant acoustic frequency). As the absorption cross-section of NO_2 displays patterns of relatively high frequencies[2], it is mandatory to adjust the frequency as a function of the ambiant temperature.

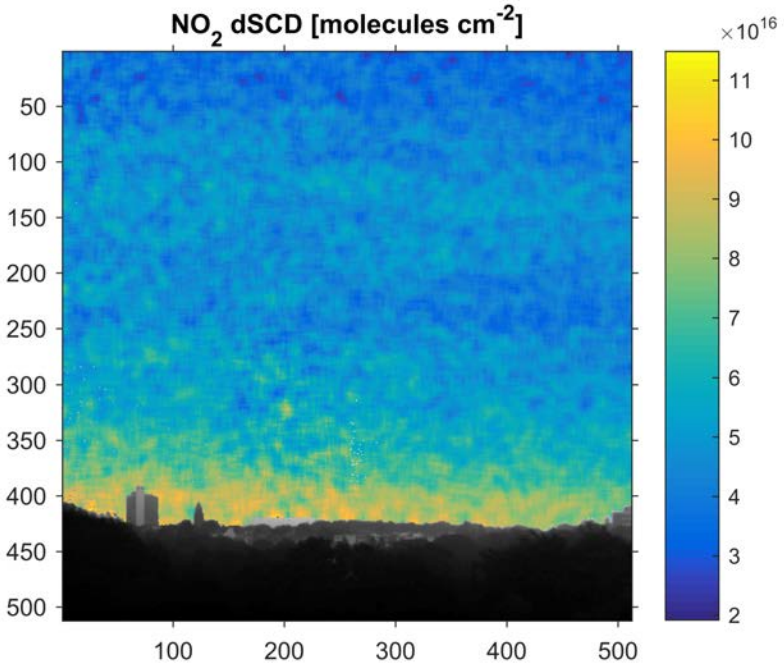

Figure 2: Map of differential slant column densities (dSCD) of NO_2 above Brussels as measured by the NO_2 camera. The x- and y-axis display the column and row number of the pixels, respectively. The colormap shows the dSCD in molecules cm^{-2}.

The increased field of view is now better suited for extended air mass monitoring, such as above cities. The new NO_2 camera was recently tested from the roof of the Royal meteorological institute of Belgium, which is located South of Brussels. By pointing the instrument towards the North, one can observe the air mass above the city center, a highly polluted one. Figure **2** shows a typical result: a map of the differential slant column density (dSCD) of NO_2, as inferred from the spectral irradiance observed by each pixel. This is a measure of the relative abundance of NO_2 over the light path seen by a pixel compared to a reference light path subject to much less concentrations of NO_2 (generally above the region of interest). Such a spatial resolution has never been achieved by horizon-looking grating-based instruments, even the scanning ones: at a distance of 5 km, the new NO_2 camera samples the air at about 3.5 m per pixel. The next step will be to confirm the accuracy of the new NO_2 camera by comparison with a MAX-DOAS instrument.

3. MONITORING THE SOLAR SPECTRAL IRRADIANCE IN THE UV

The Sun is not only driving the Earth's energy balance, but it also plays a major role in the upper air chemistry through photo-dissociation processes. The measurement of the Solar Spectral Irradiance (SSI) from space, the absolute spectrum and its temporal variability, is fundamental for the Earth's climate system understanding as it is a primary input to the chemistry climate models (CCM) attempting to reproduce the observed changes in the atmospheric composition and circulation[8].

The continuation of SSI measurement records is fundamental for the improvement of both the solar models, and the CCMs. In particular, different patterns of variability have been observed across the recent solar cycles, and the largest uncertainties remain in explaining the temporal variability of the SSI in the UV[8].

Numerous space missions have been launched to provide SSI measurements since the late 1960's. However, none of them could reach a sufficient level of accuracy when looking at different timescales of variability but also for the absolute level of irradiance. Despite massive efforts, some key science questions about variability in the UV are still unresolved especially for long-term trends. Despite its major scientific relevance, the measurement of SSI from space is currently carried out by only one instrument, TSIS, on-board the ISS.

Prone to degradation, calibration of those instruments are extremely difficult[9]. Previous instruments were based on prisms and gratings as core light-dispersion elements, which are extremely sensitive to polymerisation of contaminant materials under solar UV exposure. These instruments require also considerably large optical paths and an important number of moving parts, which invalidate any attempt of miniaturization and optical design simplification.

It is perfectly feasible to design an AOTF-based instrument for the monitoring of the SSI variability in the UV. For its proven space qualification, and because it is transparent far in the UV, SiO_2 seems to be the best AO interaction medium. Unlike the NO_2 camera, there is no interest for hyperspectral imaging here, but an acceptance angle of at least 0.5° to match the angular diameter of the Sun, is required. Hence, a parallel tangent design[10] will be mandatory.

The spectral region 200-350 nm is probably the most important one, as the SSI variability is high[8] (up to several percents over a solar cycle at the shortest wavelengths, Figure 3), and the absorption by ozone as well. SiO_2 is transparent in this range, and a piezo-electric transducer will have to be manufactured to provide the needed tuning range based on the final AO interaction geometry. It is expected that frequencies larger than 100 MHz will be needed. A sub-nanometer spectral resolution is also desired. This will have an impact on the length of the AO interaction. In order to obtain both a large angular acceptance, and a high wavelength selectivity, a Kusters' configuration[11] could be an option.

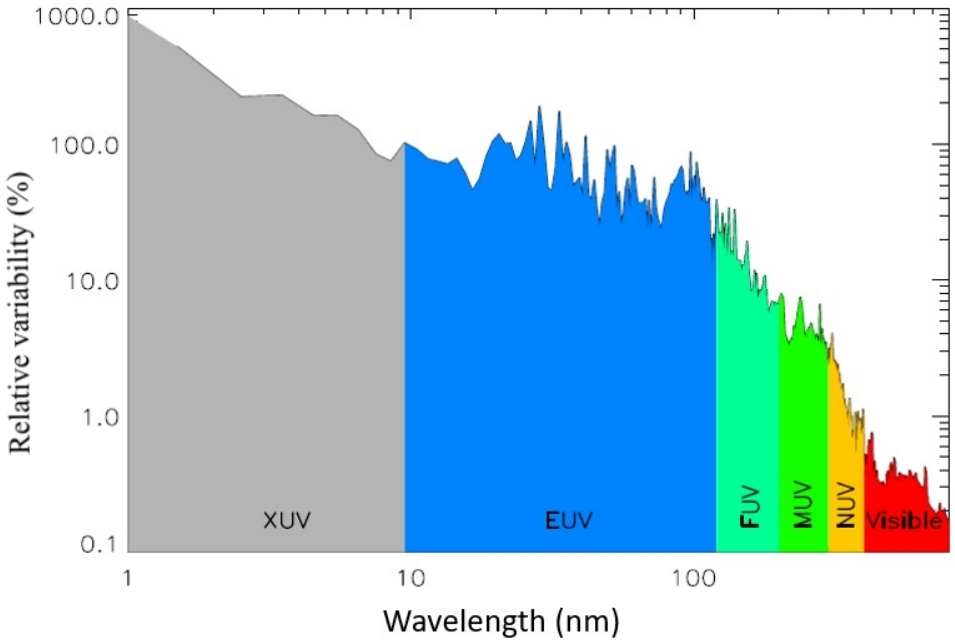

Figure 3: Relative variability of the SSI compared to solar cycle mean. Based on SORCE and TIMED data from 2003 to 2010.

Because of the small angular size of the Sun, and thanks to the acceptance angle of the AOTF, a simple instrument concept without any front-end optics appears feasible (the necessity of adding a diffuser is still being debated): a SiO_2 AOTF surrounded by two cross-oriented Glan-Taylor polarizers filtering the SSI at the desired wavelength and removing the undiffracted order, followed by a focusing lens onto a detector.

The radiometric sensitivity of a such an instrument can easily be estimated with a few basic assumptions. Let assume an effective linear aperture A = 5 mm for the AOTF. Knowing that the Sun solid angle is approximately $\Omega = 6.10^{-5}$ sr, this gives an optical throughput $G = \pi A^2\Omega/4 = 1.2x10^{-5}$ cm^2 sr. Furthermore, as the AOTF will only select one linear polarization, the irradiance will be divided by two as the solar light is unpolarized. In addition, a conservative assumption would assume a diffraction efficieny of 5% (SiO_2 has a much lower acousto-optic figure of merit than TeO_2), and a quantum efficiency of the detector of 10% at all wavelengths. Taking these values into account, and noting that the SSI varies between $0.1x10^{14}$ ph s^{-1} cm^{-2} nm^{-1} at 250 nm, and $1.8x10^{14}$ ph s^{-1} cm^{-2} nm^{-1} at 350 nm, such an instrument would provide counting rates between 10^9 e$^-$ s^{-1} and 10^{11} e$^-$ s^{-1} (1 nm bandwidth). With such high radiometric levels, a neutral density filter will probably be needed in order to not saturate the detector. On the other hand, very short exposure times will ensure rapid acquisitions (less than a minute) of the solar irradiance spectrum between 250 nm and 350 nm by steps of 0.1 nm (typical).

As can be seen, a simple AOTF-based instrument concept appears feasible for the accurate and fast acquisition of solar irradiance spectra in the UV. Thanks to the absence of FEO, such an instrument is potentially sized for a cubesat integration.

4. POLARIZED AURORAL EMISSIONS

Auroral emissions are the most spectacular display of the interactions between Earth's magnetosphere and ionosphere. The emission lines are due to de-excitation of upper atmospheric components following the impact of these particles with magnetospheric high-energy electrons precipitating along Earth's magnetic field lines. The most intense auroral emissions are the green line at 577.7 nm, the red line at 630.0 nm and the blue line at 427.8 nm. The first two are produced by oxygen atoms and peak respectively at around 110 km and 220 km altitude, while the last one is produced by N_2^+ at altitudes below 100 km.

The polarization of the 630.0 nm red line was observed for the first time by Lilensten et al.[12] using a dedicated Steerable Polarimeter (SPP). The level of polarization is of 2-3%. An example of results is shown in Figure **4**. This new observable could be useful either to monitor the response of the upper atmosphere to particle precipitations[13], to map the variations of the direction of the local magnetic field during geomagnetic activity[14], or more generally for space weather applications. Polarization is always linked to some anisotropy, either in the emission process itself or along the line-of-sight. At high latitudes, in the case of the 630 nm red line, the polarization is due to the anisotropy of the precipitating electron beams impacting oxygen atoms, creating imbalances between the various (unresolved) Zeeman sublevels[15].

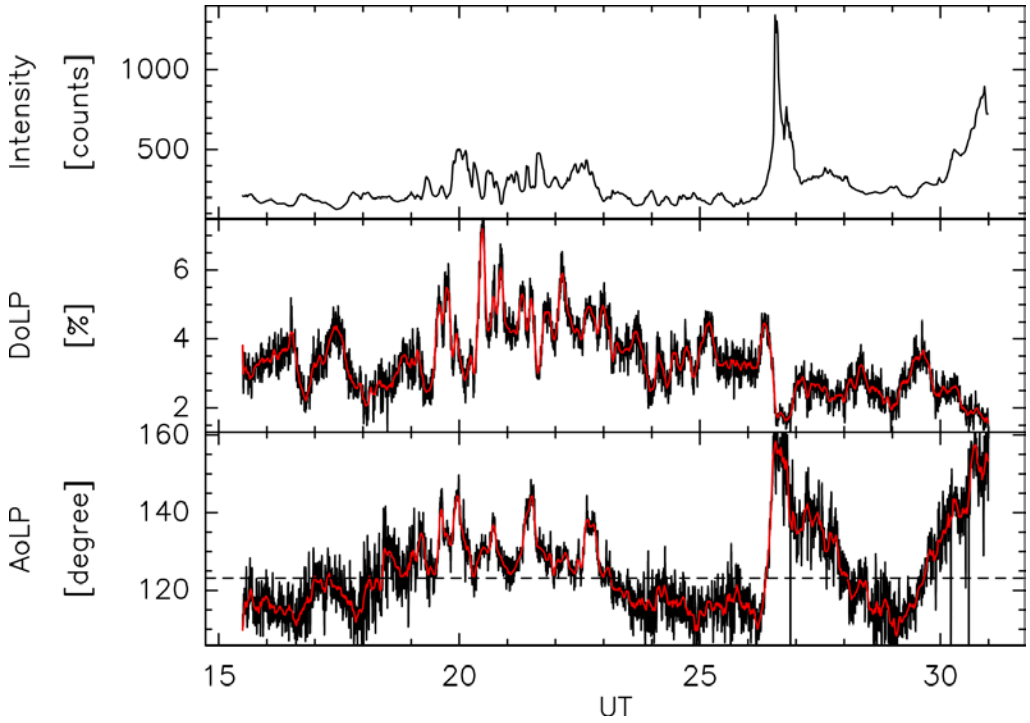

Figure 4: The SPP measurements obtained on 21 December 2014 in Ny Alesund, Svalbard, Norway. (top) The intensity of the 630.0 nm red line measured by the SPP. (middle) The Degree of Linear Polarisation (bottom), and the Angle of Linear Polarisation. The black lines are the raw data obtained with 4 s resolution. The red line is a moving average over 1 minute. The dashed horizontal line is the theoretical expected value for the angle of polarization and is equal to 123.10° [Reproduced from [14]].

The 577.7 nm green line cannot be polarized because the upper level of the transition has a total kinetic momentum J=0 and therefore no Zeeman sublevels. Therefore, among all the remaining auroral emission lines, the best candidate to study the polarization is the blue line at 427.8 nm. Additionally, it is produced only by impact with high-energy precipitating electrons while the 630.0 nm red line has also many other competing production mechanisms which are more isotropic by nature and consequently dilute the impact polarization. An attempt to measure the polarization of the blue line was made using a dedicated spectropolarimeter[16] with the goal to measure the polarization of all auroral emission lines between 400 and 700 nm. A level of a few percent of polarization was found as well but, due to weak signal-to-noise ratios, these measurements still need to be taken with caution since none of the individual data set has a detection with a 3σ confidence level. These observations need to be confirmed with an improved design to increase the signal-to-noise ratio and decrease the exposure time.

The basic requirements for an AOTF-based auroral emissions spectro-polarimeter are a spectral resolution of about 1nm (in order to resolve the structures of emission lines), a 2°x2° field of view, and a temporal resolution of a minute. Ideally, the aurora should be observed in four linear polarizations in order to retrieve the Stokes components of the light: 0°, 45°, 90°, and 135°. To achieve this, a double channel system could be designed, each channel consisting of a TeO_2 AOTF

similar to the one used in the NO_2 camera, and two photodiodes collecting the +1 and -1 orders of diffraction. The two channels baseplates should have a relative tilt angle of 45° to allow for measuring in the 4 directions of polarization. Furthermore, one could optimize the instrument to operate in a narrow band centered on the 427.8 nm line.

A basic estimation of the performance of the system can be made. Let assume an average aurora emission[17] of 1000 Rayleigh ($1R = (4\pi)^{-1}\ 10^6$ photons $s^{-1}\ cm^{-2}\ sr^{-1}$). In a telecentric optical layout, for small angles, the focal lengths of the front-end optics is given by $f = H/\phi$, where H is the linear aperture of the AOTF, and ϕ is the desired field of view. Assuming H = 10mm, and $\phi = 2°$, we find f = 286 mm, still an acceptable length for a ground based instrument. By conservation of the étendue, the diameter of the telecentric stop should be $D = f\,\Delta\theta_i$, where $\Delta\theta_i$ is the acceptance angle of the AOTF. Taking $\Delta\theta_i = 2°$ (typical for noncollinear TeO_2 AOTFs), we have D = 10 mm. The throughput of the system is given by $G = \pi D^2\Omega/4$, where $\Omega \approx 10^{-3}$ sr for a 2° field of view. With the above values, we have $G = 7.5\text{x}10^{-4}$ cm^2 sr. Accounting for a diffraction efficiency of 90%, a quantum efficiency for a standard Si detector of 50%, and a loss of about 50% for each of the orthogonal polarizations, about 20% of the collected signal is left in each diffraction order. Coming back to the 1000 R auroral emission, each detector in the proposed concept should have a count rate of about $1000.10^6/(4\pi).G.0.2 \approx 10^4$ $e^-\ s^{-1}$. An accumulation over a minute would generate a signal of $6\text{x}10^5$ e^-, a value likely sufficient to reach relative radiometric uncertainties much smaller than 1%.

5. CONCLUSIONS

We have presented three instrumental concepts dedicated to the measurement of parameters of important relevance for the atmospheric science community, though quite distant in terms of scientific domains. For each of them, the use of the AOTF provides a number of benefits:

- For the NO_2 camera, the use of an AOTF allowed to design a hyperspectral imager with a relatively large frame rate, and a large FOV, ideal for the observation of the urban air pollution. Preliminary experimental results suggest an improved spatio-temporal resolution compared to standard instruments.
- For the monitoring of the solar spectral irradiance in the UV, the proposed instrument concept is a very compact one, using a SiO_2 AOTF, two polarizers, a lens, and a detector. Assuming conservative estimates for the diffraction efficiency, we could still show an interesting radiometric sensitivity allowing the acquisition of UV solar irradiance spectra in a few tens of seconds at a 0.1 nm sampling and a high radiometric precision.
- For the measurement of the degree of linear polarization of auroral emissions, a ground-based instrument equipped with a TeO_2 AOTF was proposed. Although probably requiring a relatively long FEO (potentially reduced by optical path folding), we could confirm that the setup would provide enough radiometric sensitivity to detect average auroral emissions (1000 Rayleigh). By accumulation over a minute, the relative uncertainty on the measured signal should go well below 1%. In addition, the native polarization sensitivity of the proposed AOTF is a clear asset for this experiment.

The results obtained with the NO2 camera are very encouraging. Still, there remains some work to confirm its performance, and validate its measurements by comparison with standard instruments. The two other instrumental concepts only exist on paper, but the estimates presented here call for further elaboration, and the realization of prototypes.

REFERENCES

[1] Fussen, D., Baker, N., Debosscher, J., Dekemper, Demoulin, P., E., Errera, Q., Franssens, G., Mateshvili, N., Pereira, N., Pieroux, D. and Vanhellemont, F., "The ALTIUS atmospheric limb sounder," Journal of Quantitative Spectroscopy & Radiative Transfer, https://doi.org/10.1016/j.jqsrt.2019.06.021 (2019).

[2] Dekemper, E., Vanhamel, J., Van Opstal, B. and Fussen, D., "The AOTF-based NO2 camera," Atmos. Meas. Tech. *9*(12), 6025-6034 (2016).

[3] Elash, B. J., Bourassa, A. E., Loewen, P. R., Lloyd, N. D. and Degenstein, D. A., "The aerosol limb imager: acousto-optic imaging of limb scattered sunlight for stratospheric aerosol profiling," Atmos. Meas. Tech. 9, 1261-1277 (2016).
[4] Suhre, D. R., Denes, L. J. and Gupta, N., "Telecentric confocal optics for aberration correction of acousto-optic tunable filters," Appl. Opt. 43(6), 1255-1260 (2004).
[5] Vanhamel J., Berkenbosch S., Dekemper E., Leroux P., Neefs E. and Van Lil E., "Practical Driving Electronics for an AOTF-Based NO_2 Camera," IEEE Transactions on Instrumentation and Measurement 68(3), 874-881 (2019).
[6] Ohmachi, Y. and Uchida, N., "Temperature Dependence of Elastic, Dielectric, and Piezoelectric Constants in TeO2 Single Crystals," Journal of Applied Physics *41*(6), 2307-2311, (1970).
[7] Uchida, N., "Optical Properties of Single-Crystal Paratellurite (TeO2)," Physical Review B *4*(10), 3736-3745 (1971).
[8] Ermolli, I., et al., "Recent variability of the solar spectral irradiance and its impact on climate modelling," Atmos. Chem. Phys. *13*(8), 3945-3977 (2013).
[9] BenMoussa, A., et al., "On orbit degradation of solar instruments," Sol. Phys. 288(1), 389-434 (2013).
[10] Chang, I. C., "Noncollinear acousto-optic filter with large angular aperture," Applied Physics Letters, *25*(7), 370-372 (1974).
[11] Kusters, J. A., Wilson, D. A. and Hammond, D. L., "Optimum crystal orientation for acoustically tuned optical filters," J. Opt. Soc. Am. 64, 434-440 (1974).
[12] Lilensten, J., Moen, J., Barthélemy, M., Thissen, R., Simon, C., Lorentzen, D. A., Dutuit, O., Amblard, P. O. and Sigernes, F., "Polarization in aurorae: A new dimension for space environments studies," Geophys. Res. Lett. 35, L08804 (2008).
[13] Lilensten, J., Bommier, V., Barthélemy, M., Lamy, H., Bernard, D., Moen, J., Johnsen, M. G., Løvhaug, U. P. and Pitout, F., "The auroral red line polarisation: modelling and measurements," Journal of Space Weather and Space Climate 5(27), A26 (2015).
[14] Lilensten, J., Barthélemy, M., Besson, G., Lamy, H., Johnsen, M. G. and Moen, J., "The thermospheric auroral red line Angle of Linear Polarization," J. Geophys. Res. Space Physics 121, 7125-7134 (2016).
[15] Bommier, V., Sahal-Bréchot, S., Dubau, J. and Cornille, M., "The theoretical impact polarization of the O I 6300 Å red line of Earth aurorae," Annales Geophysicae 29, 71-79 (2011).
[16] Barthélemy, M., Lamy, H., Vialatte, A., Johnsen, M.G., Cessateur, G. and Zaourar N., "Measurement of the polarisation in the auroral N2+ 427.8 nm band," accepted for publication in Journal of Space Weather and Space Climate (2019).
[17] Rees, M. H. and Luckey, D., "Auroral electron energy derived from ratio of spectroscopic emissions 1. Model computations," *J. Geophys. Res. 79*(34), 5181-5186 (1974).